

*promoting access to White Rose research papers*



**Universities of Leeds, Sheffield and York**  
**<http://eprints.whiterose.ac.uk/>**

---

This is the author's version of a Proceedings Paper presented at the **2010 IEEE International Ultrasonics Symposium**

Arif, M, Harput, S and Freear, S (2010) *Performance Evaluation of Nonlinear Frequency Modulated Signals in Ultrasound Harmonic Imaging*. In: *Ultrasonics Symposium (IUS)*, 2010 IEEE. UNSPECIFIED. IEEE , 2016 - 2019. ISBN 978-1-4577-0382-9

White Rose Research Online URL for this paper:

<http://eprints.whiterose.ac.uk/id/eprint/76006>

---

# Performance Evaluation of Nonlinear Frequency Modulated Signals in Ultrasound Harmonic Imaging

Muhammad Arif, Sevan Harput, and Steven Freear

Ultrasound Group, School of Electronic and Electrical Engineering, University of Leeds, Leeds LS2 9JT, UK

Email: elma@leeds.ac.uk, Telephone: +44 (0) 113 343 2076, Fax: +44 (0) 113 343 2032

**Abstract**—In ultrasound harmonic imaging with linear frequency modulated (LFM) excitation, the sidelobes level in the compressed harmonic signal can be reduced by applying a windowing function. Windowing on the transmitting signal causes reduced penetration depth, whilst windowing on the receiving side results in reduced signal-to-noise ratio (SNR) gain and axial resolution. To optimize the transmitting signal energy and the SNR gain with reduced sidelobes level in the compressed harmonic signal, the use of nonlinear frequency modulated (NLFM) signals are proposed. The NLFM signal and associated second harmonic matched filter are designed using an analytical approach to minimise correlation errors. In all simulations and experiments, the NLFM signal performance is compared with the reference LFM signal of similar sweeping bandwidth and duration. The results indicate at least a 15 dB reduction in the peak sidelobes level of the NLFM compressed second harmonic signal with comparable axial mainlobe width when compared with the LFM compressed harmonic signal.

**Index Terms**—ultrasound imaging, nonlinear frequency modulation, linear frequency modulation, harmonic pulse compression.

## I. INTRODUCTION

Ultrasound imaging with the nonlinear second harmonic component (SHC) has become common in clinical practice. Ultrasound harmonic imaging provides improved axial resolution due to higher frequency and bandwidth, better lateral resolution due to narrower beam width, and reduced reverberation artifacts due to absence of the SHC at the transmitting source [1], [2].

A key issue in ultrasound harmonic imaging is the low SNR of the SHC [3]. A number of multi-pulse excitation schemes (i.e. pulse inversion, power modulation, combination of pulse inversion and power modulation, and contrast pulse sequence [4], [5]) have been proposed in order to increase the SNR of the SHC, however they are susceptible to motion artifacts and may reduce the system frame-rate [6]. Coded excitation with frequency modulated signals however offer the potential to improve the SNR of the SHC without reducing the system frame-rate and without increasing the peak acoustic pressure [7].

In this paper, NLFM signals are proposed as an excitation method to increase the SNR of the SHC and to reduce the peak sidelobes level (PSL) after pulse compression of the SHC.

## II. CODED EXCITATION

### A. Nonlinear Frequency Modulated Signals

A complex time domain chirp signal,  $x(t)$ , can be expressed as [8],

$$x(t) = p(t) e^{j2\pi \left\{ \int f_i(t) dt \right\}}, \quad 0 \leq t \leq T \quad (1)$$

where,  $p(t)$ , is the amplitude modulation function and,  $f_i$ , is the instantaneous frequency function of the chirp signal.

The NLFM signal can be designed using a numerical technique which requires a polynomial approximation for the desired instantaneous frequency function [9]. However in this paper, NLFM signal and the associated harmonic matched filter are designed using an analytical technique in order to minimize the correlation errors. The NLFM signal can also be designed without using a time domain window function by keeping the rectangular envelope of the signal which potentially increases the transmission energy and hence the SNR [10]. However, the NLFM signal is designed by modifying both amplitude and phase modulation functions to improve Doppler shift tolerance with an expense of reduced signal energy [11]. The nonlinear instantaneous frequency function,  $f_i(t)$ , of the NLFM signal is defined as [12],

$$f_{i_{NLFM}}(t) = f_c + \frac{B}{2} \left[ \frac{\alpha \tan\left(\frac{2\gamma t}{T}\right)}{\tan(\gamma)} + \frac{2(1-\alpha)t}{T} \right] \quad (2)$$

where  $B$  is the total sweep bandwidth,  $T$  is the duration, and  $f_c$  is the centre frequency of the chirp signal. The parameters  $\alpha$  and  $\gamma$  are used to control the nonlinear FM curve.

The amplitude modulation function,  $p(t)$ , of the NLFM signal can be expressed as,

$$p(t) \approx \sqrt{|X(f)|^2 \frac{d}{dt} \{f_i(t)\}} \quad (3)$$

where  $|X(f)|^2$  is the power spectrum of the chirp signal  $x(t)$ . In the design process of the NLFM signal, a Hann window is selected as a desired shape of the power spectrum in order to obtain reduced sidelobes level after pulse compression.

Finally, the NLFM signal can be get by substituting the  $p(t)$  and  $f_{i_{NLFM}}(t)$  from (3) and (2) into (1).

## B. Linear Frequency Modulated Signals

In all simulations and experiments, the performance of the NLFM signal is compared with the LFM signal. The instantaneous frequency function,  $f_{i_{LFM}}(t)$ , of the LFM signal can be expressed as,

$$f_{i_{LFM}}(t) = \frac{B}{T}t + f_c - \frac{B}{T} \quad (4)$$

The LFM signal can be obtained by substituting the,  $f_{i_{LFM}}(t)$ , into (1).

The NLFM and LFM excitation signals are designed with a centre frequency ( $f_c$ ) of 2.25 MHz, duration ( $T$ ) of 20  $\mu$ s, and a -6 dB fractional bandwidth of 20%. A 10% tapered cosine window is also applied to the LFM signal to reduce spectral ripples. The NLFM signal parameters  $\alpha = 0.4$  and  $\gamma = 1.2$  are chosen to get the desired shape of the power spectrum that matches the transfer function of the ultrasound transducer and also contain less spectral ripples. The instantaneous frequencies of NLFM and LFM signals are shown in Fig. 1. The designed excitation signals and the associated power spectra are shown in Fig. 2.

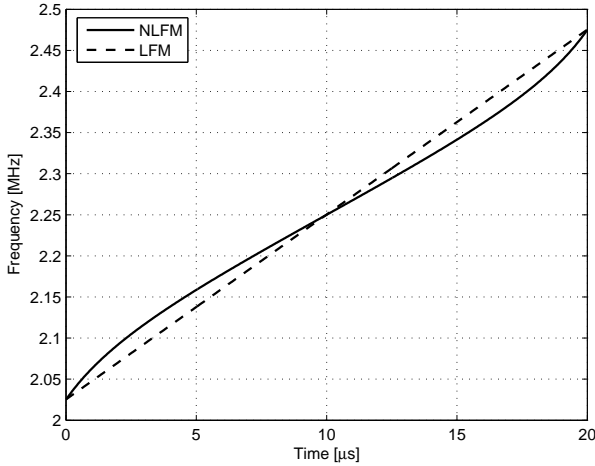


Fig. 1. The figure shows the instantaneous frequency curves of the NLFM (solid line) and LFM (dashed line) signals.

The harmonic matched filter (HMF) is proposed to process the nonlinear received signals and to perform second harmonic pulse compression. The HMF is designed by doubling the centre frequency and bandwidth parameters of the excitation chirp signal [13]. Because the less tapering is applied to the LFM signal, the harmonic mismatched filter (HMMF) is proposed to perform pulse compression of the SHC and to further reduce the sidelobes level in the LFM compressed second harmonic signal. The HMMF is designed by the application of a Chebyshev window of 80 dB attenuation to the HMF. The power spectrum of the designed HMF and HMMF are shown in Fig. 3.

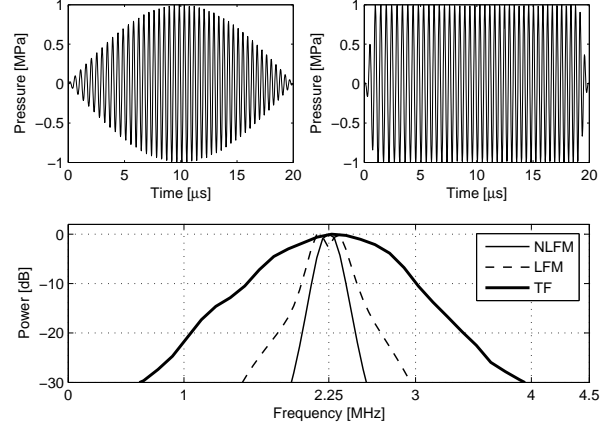


Fig. 2. Illustration of the NLFM signal (top, left), reference LFM signal (top, right), the corresponding power spectra of the excitation signals and the transfer function (TF) of the ultrasound transducer used in the experiments (bottom).

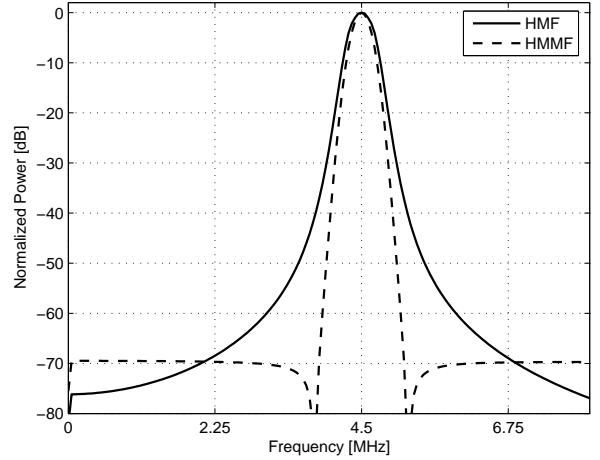


Fig. 3. The figure shows the power spectrum of the designed harmonic matched filter (solid line) and harmonic mismatched filter (dashed line) for second harmonic pulse compression.

## III. MATERIALS AND METHODS

### A. Simulations

The generation of higher order harmonic components due to the nonlinear propagation of the ultrasound wave through medium is simulated using the ‘ $B/A$ ’ model [14].

$$\rho \frac{\partial^2 u}{\partial t^2} = -\nabla p, \quad p = -\rho c^2 \left( \nabla \cdot u + \frac{1}{2} \frac{B}{A} (\nabla \cdot u)^2 \right) \quad (5)$$

where  $u$  is the particle displacement vector,  $p$  is the acoustic pressure,  $\rho$  is the material density,  $c$  is the speed of sound, and  $B/A$  is the nonlinear coefficient. The model is simulated in Matlab where the simulation parameters are shown in Table I.

TABLE I  
PARAMETERS USED IN SIMULATIONS

Parameters	Symbol	Value / Unit
Peak acoustic pressure	$p$	1 MPa
Axial distance	$z$	50 mm
Material density	$\rho$	1000 kg/m <sup>3</sup>
Speed of sound	$c$	1500 m/s
Nonlinear coefficient	$B/A$	5.2
Frequency dependent attenuation	$\alpha$	0.5 dB/[cm×MHz]

### B. Experiments

The experimental setup for measuring the harmonic components due to nonlinear propagation of ultrasound waves through water is shown in Fig. 4. The transducer and hydrophone are mounted coaxially in a pitch-catch configuration and aligned at a depth of 50 mm using a custom built motion control system. A programmable function generator (33250A Agilent, 80 MHz, Santa Clara, CA, USA) is programmed to generate the designed NLFM and LFM excitation signals. The generated signals are amplified by a linear power amplifier (A150 E&I, 55 dB, Rochester, NY, USA) and transmitted by a 2.25 MHz single element transducer (56% fractional bandwidth, V323-SM, Panametrics, Waltham, MA, USA). The signals are received using a 0.2 mm needle-type (Polyvinylidene Fluoride) PVDF hydrophone (calibrated from 1 to 20 MHz, Precision Acoustics Ltd., Dorchester, UK). The pressure level of each waveform is calibrated and the mechanical index (MI) of 0.2 (peak negative pressure of 300 kPa at 2.25 MHz) is set at the receiver. The received signals are acquired at 1 GHz using a digital oscilloscope (44Xi LeCroy, 400 MHz, Chestnut Ridge, NY, USA) with 32 times averaging. The data is stored in a computer and processed offline using MATLAB software (The MathWorks Inc., Natick, MA, USA). The received signals are corrected using an inverse filter which is designed according to the frequency response of the needle hydrophone.

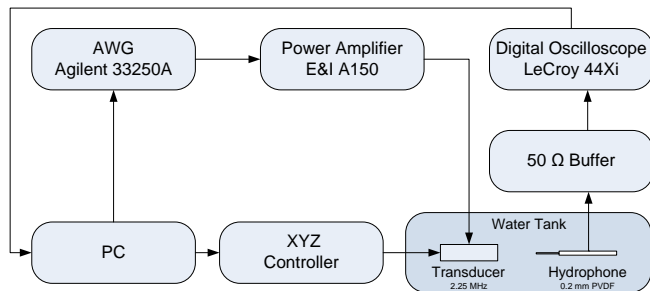


Fig. 4. Schematic diagram of the experimental setup.

## IV. RESULTS AND DISCUSSION

### A. Simulations

The simulation results are shown in Fig. 5. The spectra of the received signals show the existence of the SHC which is 20 dB below the fundamental component.

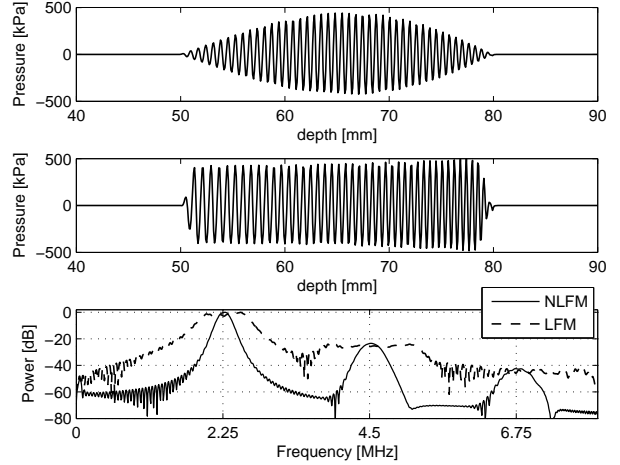


Fig. 5. Illustration of the simulated NLFM (top), and LFM (middle) nonlinear signals received at a depth of 50 mm, and the corresponding power spectra of the received signals (bottom).

The pulse compression results of the simulated SHC signals are shown in Fig. 6. The pulse compression parameters are shown in Table II. The results indicate a 18 dB reduction of the PSL in the compressed second harmonic NLFM signal when compared with the compressed second harmonic signal of the LFM. Also the -20 dB mainlobe width (MLW) of the NLFM compressed SHC is reduced by 30% when compared with the MLW of the LFM compressed signal.

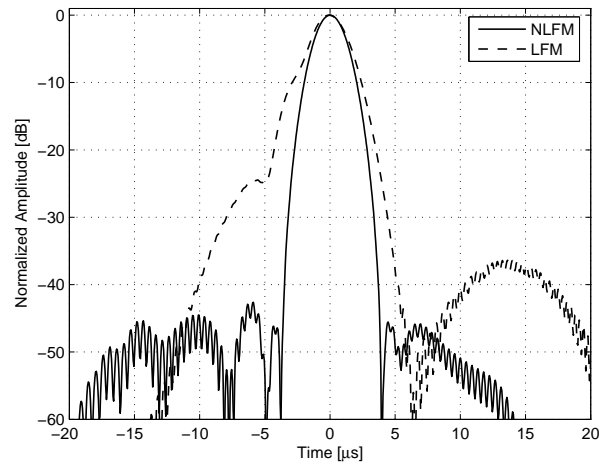


Fig. 6. The figure shows the pulse compression of the simulated NLFM (solid line) and LFM (dashed line) second harmonic signals.

## B. Experiments

The nonlinear signals received at a depth of 50 mm are shown in Fig. 7. It is shown that the SNR of the received NLFM signal is similar to the LFM signal even though the energy of the transmitted NLFM signal was 54% of the LFM signal. The -6 dB bandwidth of the SHC when excited with LFM is higher than the NLFM because less tapering was used in the design process of the LFM excitation signal. Also the LFM SHC contains higher ripples than the NLFM SHC.

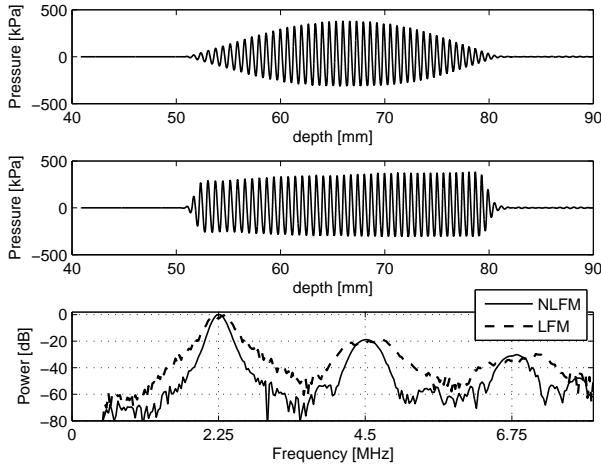


Fig. 7. Illustration of the measured NLFM (top), and LFM (middle) nonlinear signals received at a depth of 50 mm, and the corresponding power spectra of the received signals (bottom).

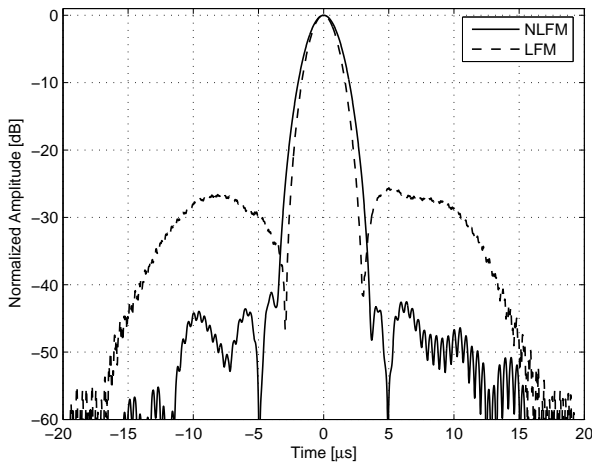


Fig. 8. The figure shows the pulse compression of the measured NLFM (solid line) and LFM (dashed line) second harmonic signals.

The second harmonic pulse compression of the measured nonlinear signals is shown in Fig. 8. The results indicate a 15 dB reduction of the PSL in the compressed SHC when using an NLFM excitation signal compared to LFM. The MLW of the NLFM compressed signal is slightly higher than the LFM

compressed signal, this is due to different bandwidth levels between the LFM and NLFM.

TABLE II  
PERFORMANCE EVALUATION PARAMETERS OF SECOND HARMONIC PULSE COMPRESSION

	Simulations		Experiments	
	MLW [ $\mu$ s]	PSL [dB]	MLW [ $\mu$ s]	PSL [dB]
NLFM	5.5	-42.6	5.4	-41.1
LFM	7.8	-24.4	4.6	-25.5

## V. CONCLUSION

In this paper, NLFM signals are proposed as an excitation method in order to increase the SNR and to reduce the PSL after pulse compression of the SHC. The signal energy can be efficiently transmitted using the NLFM signal by matching the signal spectrum to the transfer function of the ultrasound transducer. This results in an improved SNR and reduced ripples in the SHC of the received signal. Moreover, no additional windowing is required on the HMF to reduce the PSL of the compressed SHC signal.

## REFERENCES

- [1] R. S. C. Cobbold, *Foundations of Biomedical Ultrasound*. New York, NY, USA: Oxford University Press, 2007.
- [2] F. A. Duck, "Nonlinear acoustics in diagnostic ultrasound," *Ultrasound in Medicine & Biology*, vol. 28, no. 1, pp. 1 – 18, 2002.
- [3] M. Averkiou, "Tissue harmonic imaging," in *Ultrasonics Symposium, 2000 IEEE*, vol. 2, Oct 2000, pp. 1563–1572.
- [4] M. A. Averkiou, C. Mannaris, M. Bruce, and J. Powers, "Nonlinear pulsing schemes for the detection of ultrasound contrast agents," *Acoustical Society of America Journal*, vol. 123, pp. 915–920, 2008.
- [5] P. Phillips, "Contrast pulse sequences (cps): imaging nonlinear microbubbles," in *Ultrasonics Symposium, 2001 IEEE*, vol. 2, 2001, pp. 1739 –1745.
- [6] C.-C. Shen and P.-C. Li, "Motion artifacts of pulse inversion-based tissue harmonic imaging," *Ultrasonics, Ferroelectrics and Frequency Control, IEEE Transactions on*, vol. 49, no. 9, pp. 1203–1211, Sep 2002.
- [7] R. Arshadi, A. C. H. Yu, and R. S. C. Cobbold, "Coded excitation methods for ultrasound harmonic imaging," *Canadian Acoustics*, vol. 35, no. 2, pp. 35–46, 2007.
- [8] T. Misaridis and J. Jensen, "Use of modulated excitation signals in medical ultrasound. part ii: design and performance for medical imaging applications," *Ultrasonics, Ferroelectrics and Frequency Control, IEEE Transactions on*, vol. 52, no. 2, pp. 192–207, Feb. 2005.
- [9] F. Gran and J. Jensen, "Designing waveforms for temporal encoding using a frequency sampling method," *Ultrasonics, Ferroelectrics and Frequency Control, IEEE Transactions on*, vol. 54, no. 10, pp. 2070–2081, October 2007.
- [10] R. Milleit, "A matched-filter pulse-compression system using a nonlinear fm waveform," *Aerospace and Electronic Systems, IEEE Transactions on*, vol. AES-6, no. 1, pp. 73–78, Jan. 1970.
- [11] J. Johnston and A. Fairhead, "Waveform design and doppler sensitivity analysis for nonlinear fm chirp pulses," *Communications, Radar and Signal Processing, IEE Proceedings F*, vol. 133, no. 2, pp. 163–175, April 1986.
- [12] T. Collins and P. Atkins, "Nonlinear frequency modulation chirps for active sonar," *Radar, Sonar and Navigation, IEE Proceedings -*, vol. 146, no. 6, pp. 312–316, Dec 1999.
- [13] J. M. G. Borsboom, C. T. Chin, and N. de Jong, "Nonlinear coded excitation method for ultrasound contrast imaging," *Ultrasound in Medicine & Biology*, vol. 29, no. 2, pp. 277–284, 2003.
- [14] M. Anderson, "A 2d nonlinear wave propagation solver written in open-source matlab code," in *Ultrasonics Symposium, 2000 IEEE*, vol. 2, oct 2000, pp. 1351 –1354.